HHS Public Access

Author manuscript

Ultrason Imaging. Author manuscript; available in PMC 2017 May 01.

Published in final edited form as:

Ultrason Imaging. 2016 May ; 38(3): 194–208. doi:10.1177/0161734615589252.

Improved Correlation of Strain Indices with Cognitive Dysfunction with Inclusion of Adventitial Layer with Carotid Plaque

X. Wang[1], **C. C. Mitchell**[2], **T. Varghese**[1], **D. C. Jackson**[3], **B. G. Rocque**[4], **B. P. Hermann**[3], and **R. J. Dempsey**[4]

[1]Department of Medical Physics, University of Wisconsin–Madison School of Medicine and Public Health, Madison, WI, USA

[2]Department of Medicine, University of Wisconsin–Madison, Madison School of Medicine and Public Health, WI, USA

[3]Department of Neurology, University of Wisconsin–Madison, Madison School of Medicine and Public Health, WI, USA

[4]Department of Neurological Surgery, University of Wisconsin–Madison School of Medicine and Public Health, Madison, WI, USA

Abstract

Plaque instability may lead to chronic embolization, which in turn may contribute to progressive cognitive decline. Accumulated strain tensor indices over a cardiac cycle within a pulsating carotid plaque may be viable biomarkers for the diagnosis of plaque instability. Using plaque-only carotid artery segmentations, we recently demonstrated that impaired cognitive function correlated significantly with maximum axial and lateral strain indices within a localized region of interest in plaque. Inclusion of the adventitial layer focuses our strain or instability measures on the vessel wall-plaque interface hypothesized to be a region with increased shearing forces and measureable instability. A hierarchical block-matching motion tracking algorithm developed in our laboratory was used to estimate accumulated axial, lateral, and shear strain distribution in plaques identified with the plaque-with-adventitia segmentation. Correlations of strain indices to the Repeatable Battery for the Assessment of Neuropsychological Status Total score were performed and compared with previous results. Overall, correlation coefficients (r) and significance (p) values improved for axial, lateral, and shear strain indices. Shear strain indices, however, demonstrated the largest improvement. The Pearson correlation coefficients for maximum shear strain and cognition improved from the previous plaque-only analyses of −0.432 and −0.345 to −0.795 and −0.717 with the plaque-with-adventitia segmentation for the symptomatic group and for all patients combined, respectively. Our results demonstrate the advantage of including adventitia for ultrasound carotid strain imaging providing improved association to parameters assessing

Corresponding Author: T. Varghese, Department of Medical Physics, University of Wisconsin–Madison School of Medicine and Public Health, Madison, WI 53706, USA. tvarghese@wisc.edu.

Declaration of Conflicting Interests

The author(s) declared no potential conflicts of interest with respect to the research, authorship, and/or publication of this article.

cognitive impairment in patients. This supports theories of the importance of the vessel wall plaque interface in the pathophysiology of embolic disease.

Keywords

elasticity imaging; carotid plaque; motion tracking; strain; vascular cognitive dementia

Introduction

Microemboli generated from the rupture of vulnerable carotid plaque can flow into the vasculature of the brain and cause ischemic events resulting in stroke, vascular cognitive impairment, or both.[1] For every patient suffering a stroke, twice as many people experience vascular cognitive impairment,[2] and five times more may undergo “silent” strokes.[3] It is likely that these “silent” strokes may be associated with accumulated cognitive decline. The pathophysiology of silent strokes includes microvascular degeneration, either in the brain or in the feeding vessel walls, and embolic disorders.[4,5] In this paper, we focus on the possibility of physical abnormalities within diseased carotid vessels as measurable markers of microvascular pathology and potential sources of microemboli.[6,7] Studies have suggested that silent strokes may occur with concurrent subclinical microemboli[8] and have been associated with cognitive impairment.[9] Vascular cognitive impairment,[10] in contrast, may be predicted by arterial aging and stiffening.[11] Generally, carotid endarterectomies (CEA) are performed on patients when the stenosis is greater than 70%, regardless of the plaque composition.[12] Carotid stenosis by itself may not result in emboli; how-ever, the structural stability of the deposited plaque is a more direct indicator of emboli. In our analysis, softer plaques that are prone to increased deformations over a cardiac cycle are hypothesized to be vulnerable and predisposed to shedding emboli. There is evidence that cerebral microemboli have a significant correlation with vascular dementia and are associated with a faster decline of cognitive function.[13,14] Correlations have also been found between the number of intra-operative microemboli detected by trans-cranial Doppler and the post-operational cognitive measures.[15-17]

Ultrasound elasticity imaging has been widely investigated in assessing plaque vulnerability,[8,18-23] and may assist in the prediction of embolism and resulting stroke or cognitive impairment. In noninvasive ultrasound strain imaging, Lagrangian strain estimation has shown better perfor- mance than an Eulerian approach for short-axes view of the heart.[24] A Lagrangian speckle model for strain estimation on plaque was developed to estimate axial, lateral, shear, and radial strain and to characterize mechanical properties of the vessel wall.[25] This model was later implemented to calculate strain tensors on both cross-sectional and longitudinal imaging views to assess axial strain and axial shear strain.[26] In our laboratory, a robust strain estimation algorithm using a Lagrangian description was also developed to estimate all components of the strain tensor.[27] Accumulated strain indices derived from the strain tensor were used to assess the vulnerability of carotid plaque based on increased deformation over a cardiac cycle.[28,29]

It has been reported that increased axial and lateral strain in plaque[28] may correlate with cognitive abnormalities,[29,30] suggesting that it is important to identify patients with unstable or vulnerable plaques to help prevent future silent strokes and cognitive impairment. However, Wang et al.[29] found no significant correlation of shear strain indices with cognitive function if the strain was measured as representative of the entire plaque sample. As shear stress may develop at the interface between different tissue constituents with different stiffness inside the plaque,[31] shear strain may be an important indicator in the pathogenesis of plaque rupture.[32] It has been previously reported that the shear strain in the adventitia of the common carotid artery has a cyclic behavior, induced by the pulsating blood pressure.[22] Other studies have shown that the intima-media layer in the vessel wall may have longitudinal movements that can also cause shear strain in the adventitia.[33] We have also shown previously that there are high strain values at the plaque-adventitia interface during lateral motion in a human carotid artery.[27,28]

In our previous work, the adventitia layer was not included with the plaque region during segmentation process (i.e., plaque-only segmentation). Recently, we observed large shear strains in the carotid artery wall in volunteers. Therefore, in this paper, we include adventitia also in the segmentation (i.e., plaque-with-adventitia segmentation) based on the hypothesis that high shear strains may be present in the adventitial layer or at the plaque-adventitia interface. The plaque-with-adventitia segmentation method not only takes the shearing at plaque boundaries into account, but also is an easier and more convenient method for radiologists because it is difficult to distinguish plaque from adventitia in ultrasound B-mode images in many instances. For the plaque-only method, intima-media was also included as it is almost inseparable from plaque. We compare the strain indices obtained with the inclusion of the adventitial layer and their correlations to cognitive function in human subjects to our previous results.

Materials and Method

The study was performed on the same group of 24 patients who presented with significant plaque in our previous work.[29] Ultrasound and strain imaging was performed before the CEA procedure at the University of Wisconsin–Madison Hospitals and Clinics. Informed consent using a protocol approved by the University of Wisconsin–Madison Institutional Review Board (IRB) was provided by patients prior to the ultrasound and strain imaging study. Patients ranged in age from 44 to 79, with a mean age of 65.88 ± 8.74, respectively. Sixteen patients were male, and 8 were female, but no sex-based differences were present. The 24 patients were assigned to 3 groups: 16 symptomatic, 7 asymptomatic, and 1 uncertain. The patients who presented with stroke or transient ischemic attack (TIA) were classified as symptomatic. Asymptomatic patients without TIA could have carotid stenosis and indication for CEA based on other clinical symptoms or imaging studies performed; for example, patients presenting with cardiac conditions. Further details on these participants is available in the previous paper.[29] In addition to patients, a healthy volunteer was also scanned. Informed consent using a protocol approved by the University of Wisconsin–Madison IRB was obtained from the volunteer prior to the ultrasound and strain imaging study.

A Siemens Antares ultrasound system (Siemens Ultrasound, Mountain View, CA, USA) equipped with a VFX 13-5 linear transducer was used to acquire radiofrequency (RF) echo signal data, clinical B-mode images, and color-flow Doppler images. The depth of the B-mode image was 4 cm, and the lateral width was 3.8 cm that included 508 A-lines. A single transmit focus was set at the depth of plaque with a transmit frequency of 11.4 MHz and a sampling frequency of 40 MHz.

Plaque regions with adventitia were segmented by a radiologist on the B-mode images constructed from RF data, as shown in Figure 1. Two complete cardiac cycles were chosen, with plaque segmentation performed on the three end-diastolic frames using the Medical Imaging Interaction Toolkit (MITK). Clinical B-mode and color-flow Doppler images were also used by the radiologist in determining the boundary of plaque. In the previous work, we used the plaque-only segmentation (i.e., plaque is separated from artery wall on the plaque-adventitia interface), as shown in Figure 1(b). In this paper, we propose including the adventitia layer in the demarcation of plaque, denoted as the plaque-with-adventitia segmentation in Figure 1(c).

We used a hierarchical block-matching motion tracking algorithm developed in our laboratory[27] to estimate subsample[34] accumulated axial, lateral, and shear strain distribution in plaques identified with the plaque-with-adventitia segmentation. Displacements between pre- and post-deformation frames were tracked with a three-level block-matching technique. The matching block was 15 × 28 pixels at the top level and 10 × 18 pixels at the bottom level, with no overlap between the blocks. Along the axial direction, 1 pixel represents 0.02mm, while along the lateral direction 1 pixel represents 0.075mm. Normalized cross-correlation analysis was performed using recursive Bayesian regularization over three iterations to improve the quality of the tracked displacements at each level for both axial and lateral displacements.[35] A dynamic frame skip method was used to obtain optimal motion tracking over a cardiac cycle, with a short frame skip during systole and a long frame skip during end diastole. The threshold for frame skip was an absolute axial strain of 5% inside a subregion of the image. Incremental local displacements were then estimated in each frame and filtered with a 3 × 3 pixel median filter to remove outliers. Finally, local strain was assessed by applying a modified least-squares fit over a 7 pixel length from displacement estimation accumulated over a cardiac cycle using the end-diastolic frame as the reference frame. In this work, shear strain was computed by the equation $e_{xy} = ½(\delta d_y/\delta x + \delta d_x/\delta y)$, where x and y represent the lateral and axial directions, respectively.[27] Displacements and strains between consecutive frames calculated by the block-matching motion tracking algorithm were relatively small, due to the fact that the frame rates we used were no less than 27 fps. Accumulated axial, lateral, and shear strain images computed inside the segmented region were overlaid on the corresponding B-mode images and presented in Figures 2 through Figure 4. From the strain images, a small region of interest (ROI) within a 10 to 20 strain data points range with large deformations or strain in the plaque region was selected, and the strain indices were computed in this ROI. The maximum strain was defined as the maximum average strain value in this small ROI over two cardiac cycles. The corresponding minimum and peak-to-trough (previously referred to as peak-to-peak) strain indices in the same cardiac cycle were also obtained.

Cognitive assessment was also conducted before CEA using the Repeatable Battery for the Assessment of Neuropsychological Status (RBANS), which provides an index of overall cognitive status as well as five indices reflecting specific cognitive abilities (Immediate Memory, Visuospatial/Constructional, Language, Attention, and Delayed Memory).[36] All index scores are age-adjusted and normalized.[37] Ultrasound imaging and cognitive assessment were conducted separately and were blinded to each other, respectively. Strain indices were then correlated with RBANS Total scores using Pearson correlation coefficients with a two-tailed significance level of $p < 0.05$ and are compared with the correlations using a plaque-only segmentation reported previously.[29]

Results

Strain Estimate Comparisons

Figure 2 shows the comparison of axial strain images using the two segmentation methods on carotid plaque for a symptomatic patient segmented in Figure 1. Accumulated axial strain estimates overlaid on the B-mode image using the plaque-only segmentation are illustrated in Figure 2(a) and the plaque-with-adventitia segmentation in Figure 2(b). For the plaque-with-adventitia segmentation, the axial strain distribution in the adventitia is also shown in addition to the strain in the plaque. Although large accumulated axial strain values around 10% were found in the adventitia region, this did not exceed the maximum axial strain in the plaque. An asymptomatic case is also presented in Figures 2(c) and (d). The asymptomatic plaque shows less heterogeneity, but similar trends can still be observed.

In a similar manner, accumulated lateral strain images on the same symptomatic plaque with the two segmentation methods are illustrated in Figures 3(a) and (b). The extended region also has lateral strain values as large as 10%. We hypothesize that large strains in the lateral direction could arise from soft plaque deformation with blood flow, especially around stenosis. However, similar to the case with the accumulated axial strain, the maximum accumulated lateral strain does not change for the plaque even after including the adventitia layer. The asymptomatic plaque also demonstrates some large lateral strains close to adventitia, as shown in Figures 3(c) and (d).

Finally, accumulated shear strain images for the same symptomatic patient with the two segmentation methods are shown in Figures 4(a) and (b), respectively. Notice that in the extended adventitial layer, we now observe large accumulated shear strain values on the order of approximately 20% shear strain. Therefore, the maximum accumulated shear strain for this patient is located near the adventitia layer instead of within the plaque. Similarly, large shear strains were revealed after including the adventitia layer in the segmentation in the asymptomatic plaque shown in Figures 4(c) and (d). Note also that the increased accumulated shear strain in the adventitia could be due to the presence of both large accumulated axial and lateral shear strains in this region.

Variations in accumulated strain estimates after including the adventitia layer in the segmentation are demonstrated in Figure 5. Accumulated axial, lateral, and shear strains over two cardiac cycles for both plaque-only and plaque-with-adventitia segmentation on a symptomatic and asymptomatic patient are shown in Figures 5(a), (b), and (c), respectively.

Note that the absolute values of the strain increase with the inclusion of the adventitia for both symptomatic and asymptomatic patients. Accumulated axial, lateral, and shear strain plots over two cardiac cycles in the carotid artery wall of a healthy human volunteer are also shown in Figure 6(a), (b), and (c), respectively. Note that the segmented region in this case is only the vessel wall as no visible plaque was present. A cyclic variation in the accumulated strain tensor plots is clearly observed for a healthy vessel with normal blood flow. Observe the clear difference in the accumulated strain tensor estimates between that observed with a volunteer in Figure 6, versus that for patients in Figure 5. Irregular and turbulent flow patterns in the carotid arteries of patients with plaque introduce the nonperiodic patterns observed in Figure 5. Similar results have also been obtained and published by our lab on swine models.[38]

Strain and Cognition Correlations

The maximum and peak-to-trough strain indices over a small ROI with the largest deformation were obtained from the mean strain values within this ROI and then correlated with RBANS Total score. Note that the strain indices are absolute values. Figure 7 depicts the correlation of the RBANS Total score with maximum axial and lateral strain. As indicated before, the 16 symptomatic patients were plotted separately from the 7 asymptomatic patients. The uncertain one was also shown in the plot. A linear fit was performed for the two groups, respectively, and also for all patients combined. The strains in the plots are all in scalar values. Pearson coefficient (r) and significance (p) values were also obtained for each correlation. Overall, the RBANS Total score worsened with increasing strain indices for all the subjects, the same pattern identified in our previous work using plaque-only segmentation. For the maximum axial strain, the r values for the symptomatic group and for all patients combined improved from −0.533 and −0.491 to −0.569 and −0.581, respectively. For the maximum lateral strain, the r values for the symptomatic group, and for all patients combined improved from −0.650 and −0.501 to −0.760 and −0.656, respectively. The correlations for the symptomatic group and for all patients com- bined were already significant in the previous results. Still, the p value decreased. Note that $p < 0.001$ for the correlation of RBANS Total score to maximum lateral strain for the symptomatic group and for all patients combined. Minimum strain indices are not provided as we did not observe any significant improvement in the correlations for minimum strain from that described in our previous work.

The correlation of RBANS Total score with shear strain indices is illustrated in Figure 8. Here, we show both maximum and peak-to-trough shear strain indices. The correlations with the plaque-with-adventitia segmentation exhibits significant improvement when compared with the previous results. The correlation coefficients r for maximum shear strain were −0.432 and −0.345 for the symptomatic group and for all patients combined using the plaque-only segmentation, while with the plaque-with-adventitia segmentation, the correlation coefficients improved to −0.795 and −0.717. Similarly, the correlation coefficients r for peak-to-trough shear strain improved from −0.319 and −0.257 to −0.832 and −0.728 for the symptomatic group and for all patients combined. The p values also decreased, now making the correlations significant for the symptomatic group and for all

patients combined, which was not the case previously. This aspect is noteworthy because no significant correlation for shear strain indices was observed in the previous results.

A comparison of the RBANS Total scores obtained with plaque-only and plaque-with-adventitia, along with correlations to maximum accumulated strain indices, is shown in Table 1. As the correlation with RBANS Total score improved significantly with the inclusion of adventitia, we also report on the correlation of maximum accumulated strain indices to each of the component subscales of the RBANS using the plaque-with-adventitia segmentation in Table 2. Significant correlations are marked in bold. Note that the two areas of cognition that show significant correlation for the symptomatic group and for all patients combined are Immediate Memory and Delayed Memory. Immediate Memory also shows significant correlation for asymptomatic patients. For asymptomatic patients, there is also significant correlation of Attention to maximum axial strain and shear strain indices, respectively.

Discussion

Cognitive function quantified by the RBANS Total score exhibits a negative correlation with maximum accumulated axial, lateral, and shear strain indices when measured at the interface between normal adventitial wall and plaque. As the deformation or strain increases, the instability of plaque also increases concomitantly, expediting its possible rupture, resulting in embolism, and eventually leading to cognitive decline. The associations between strain and cognition reported in this work were significant for the symptomatic group and for all patients combined, suggesting a relationship between increasing strain indices in the carotid plaque and cognitive impairment through embolism. For the asymptomatic group, the correlations were not significant, partly due to the smaller size and reduced power. Despite the statistically significant correlation presented in this paper, a larger sample size is essential to further establish this relationship.

The improved strain-cognition correlation shown here supports our hypothesis that increased shear strains may exist in the adventitia layer or at the plaque-adventitia border. Our results are consistent with the evidence of shear strain in adventitia reported in the literature.[22,33] Compared with the plaque-only segmentation, the plaque-with-adventitia segmentation provides more information on the strain distribution in and around the plaque. The correlation coefficients between both the maximum accumulated axial strain and maximum lateral strain with cognitive function increased, although these changes were not as dramatic as those obtained for the accumulated shear strain indices. For the symptomatic group and for all patients combined, the maximum and peak-to-trough shear strain indices demonstrated significant correlation with cognitive function after including adventitia, which suggests that large shear strain values in the adventitia should be considered in the characterization of carotid plaque. These results also suggest that plaque residual wall interface is of importance in the etiology of a symptomatic disorder, just as they suggest that carotid plaque instability is an important etiology of cognitive vascular decline.

Shear strain within the arterial wall has been studied extensively as it may be responsible for plaque formation and rupture. As people age, their artery walls stiffen, and thus, the shear

strain may also increase between the vascular arterial layers. The adventitia layer is associated with plaque progression and thrombus formation because angiogenesis, a possible factor in facilitating plaque rupture, originates from adventitia-media interface.[39-42] Significant shear can occur between adventitia and media, resulting in the tearing of the vasa vasorum, which arises from the adventitia to supply the media layer. Rupture of vasa vasorum can produce microhemorrhage into a plaque, leaving fissures that can cause instability, local thrombosis, and embolism.[43-45]

Conclusion

The results demonstrate the feasibility and advantage of the plaque-with-adventitia segmentation method over the plaque-only segmentation method. The significant correlations between cognitive function and maximum axial, lateral, and shear strain indices suggest that ultrasound strain imaging may be a useful tool in the prediction of embolism and resulting cognitive impairment. As this is the interface of microvascular abnormalities essential for plaque growth and instability, it is likely to be the area where one could most easily noninvasively image for plaque instability using these techniques.

Acknowledgments

The authors would like to thank Ms. Pamela Winne for coordinating the data acquisition on patients.

Funding

The author(s) disclosed receipt of the following financial support for the research, authorship, and/or publication of this article: This work was supported in part by National Institutes of Health (NIH) Grants R21 EB010098-02, R01 NS064034-05, and 2R01 CA112192-06. This research was performed using the computational resources provided by the University of Wisconsin (UW)–Madison Center for High Throughput Computing (CHTC) in the Department of Computer Sciences. The CHTC is supported by UW–Madison and the Wisconsin Alumni Research Foundation, and is an active member of the Open Science Grid, which is supported by the National Science Foundation and the U.S. Department of Energy's Office of Science.

References

1. Whisnant JP, Basford JR, Bernstein EF, Cooper ES, Dyken ML, Easton JD, et al. Special report from the National Institute of Neurological Disorders and Stroke. Classification of cerebrovascular diseases III. Stroke. 1990; 21:637–76. [PubMed: 2326846]
2. Hachinski V, Iadecola C, Petersen RC, Breteler MM, Nyenhuis DL, Black SE, et al. National Institute of Neurological Disorders and Stroke—Canadian Stroke Network vascular cognitive impairment harmonization standards. Stroke. 2006; 37:2220–41. [PubMed: 16917086]
3. Vermeer SE, Prins ND, den Heijer T, Hofman A, Koudstaal PJ, Breteler MM. Silent brain infarcts and the risk of dementia and cognitive decline. N Engl J Med. 2003; 348:1215–22. [PubMed: 12660385]
4. Fleg JL, Stone GW, Fayad ZA, Granada JF, Hatsukami TS, Kolodgie FD, et al. Detection of high-risk atherosclerotic plaque: report of the NHLBI Working Group on current status and future directions. JACC Cardiovasc Imaging. 2012; 5:941–55. [PubMed: 22974808]
5. AlMuhanna K, Zhao L, Kowalewski G, Beach KW, Lal BK, Sikdar S. Investigation of cerebral hemodynamics and collateralization in asymptomatic carotid stenoses. Conf Proc IEEE Eng Med Biol Soc. 2012:5618–21. [PubMed: 23367203]
6. Fleiner M, Kummer M, Mirlacher M, Sauter G, Cathomas G, Krapf R, et al. Arterial neovascularization and inflammation in vulnerable patients: early and late signs of symptomatic atherosclerosis. Circulation. 2004; 110:2843–50. [PubMed: 15505090]

7. Tureyen K, Vemuganti R, Salamat MS, Dempsey RJ. Increased angiogenesis and angiogenic gene expression in carotid artery plaques from symptomatic stroke patients. Neurosurgery. 2006; 58:971–7. discussion 971-7. [PubMed: 16639334]
8. Dempsey RJ, Vemuganti R, Varghese T, Hermann BP. A review of carotid atherosclerosis and vascular cognitive decline: a new understanding of the keys to symptomology. Neurosurgery. 2010; 67:484–93. discussion 93-4. [PubMed: 20644437]
9. Elias MF, Sullivan LM, D'Agostino RB, Elias PK, Beiser A, Au R, et al. Framingham stroke risk profile and lowered cognitive performance. Stroke. 2004; 35:404–9. [PubMed: 14726556]
10. O'Brien JT, Erkinjuntti T, Reisberg B, Roman G, Sawada T, Pantoni L, et al. Vascular cognitive impairment. Lancet Neurol. 2003; 2:89–98. [PubMed: 12849265]
11. Gorelick PB, Scuteri A, Black SE, Decarli C, Greenberg SM, Iadecola C, et al. Vascular contributions to cognitive impairment and dementia: a statement for healthcare professionals from the American Heart Association/American Stroke Association. Stroke. 2011; 42:2672–713. [PubMed: 21778438]
12. Hanley D, Gorelick PB, Elliott WJ, Broder MS, Saver JL, Kidwell CS, et al. Determining the appropriateness of selected surgical and medical management options in recurrent stroke prevention: a guideline for primary care physicians from the National Stroke Association work group on recurrent stroke prevention. J Stroke Cerebrovasc Dis. 2004; 13:196–207. [PubMed: 17903976]
13. Purandare N, Voshaar RC, Hardicre J, Byrne J, McCollum C, Burns A. Cerebral emboli and depressive symptoms in dementia. Br J Psychiatry. 2006; 189:260–3. [PubMed: 16946362]
14. Purandare N, Voshaar RC, Morris J, Byrne JE, Wren J, Heller RF, et al. Asymptomatic spontaneous cerebral emboli predict cognitive and functional decline in dementia. Biol Psychiatry. 2007; 62:339–44. [PubMed: 17531959]
15. Russell D. Cerebral microemboli and cognitive impairment. J Neurol Sci. 2002; 203(4):211–4. [PubMed: 12417386]
16. Stump DA, Rogers AT, Hammon JW, Newman SP. Cerebral emboli and cognitive outcome after cardiac surgery. J Cardiothorac Vasc Anesth. 1996; 10:113–8. quiz 8-9. [PubMed: 8634376]
17. Braekken SK, Reinvang I, Russell D, Brucher R, Svennevig JL. Association between intraoperative cerebral microembolic signals and postoperative neuropsychological deficit: comparison between patients with cardiac valve replacement and patients with coronary artery bypass grafting. J Neurol Neurosurg Psychiatry. 1998; 65:573–6. [PubMed: 9771790]
18. Varghese T. Quasi-static ultrasound elastography. Ultrasound Clin. 2009; 4:323–38. [PubMed: 20798841]
19. Kim K, Huang SW, Hall TL, Witte RS, Chenevert TL, O'Donnell M. Arterial vulnerable plaque characterization using ultrasound-induced thermal strain imaging (TSI). IEEE Trans Biomed Eng. 2008; 55:171–80. [PubMed: 18232359]
20. Korukonda S, Nayak R, Carson N, Schifitto G, Dogra V, Doyley MM. Noninvasive vascular elastography using plane-wave and sparse-array imaging. IEEE Trans Ultrason Ferroelectr Freq Control. 2013; 60:332–42. [PubMed: 23357907]
21. Doherty JR, Dumont DM, Trahey GE, Palmeri ML. Acoustic radiation force impulse imaging of vulnerable plaques: a finite element method parametric analysis. J Biomech. 2013; 46:83–90. [PubMed: 23122224]
22. Idzenga T, Holewijn S, Hansen HH, de Korte CL. Estimating cyclic shear strain in the common carotid artery using radiofrequency ultrasound. Ultrasound Med Biol. 2012; 38:2229–37. [PubMed: 23062371]
23. Shi H, Varghese T. Two-dimensional multi-level strain estimation for discontinuous tissue. Phys Med Biol. 2007; 52:389–401. [PubMed: 17202622]
24. Ma C, Varghese T. Lagrangian displacement tracking using a polar grid between endocardial and epicardial contours for cardiac strain imaging. Med Phys. 2012; 39:1779–92. [PubMed: 22482601]
25. Maurice RL, Ohayon J, Fretigny Y, Bertrand M, Soulez G, Cloutier G. Noninvasive vascular elastography: theoretical framework. IEEE Trans Med Imaging. 2004; 23:164–80. [PubMed: 14964562]

26. Schmitt C, Soulez G, Maurice RL, Giroux MF, Cloutier G. Noninvasive vascular elastography: toward a complementary characterization tool of atherosclerosis in carotid arteries. Ultrasound Med Biol. 2007; 33:1841–58. [PubMed: 17698283]
27. McCormick M, Varghese T, Wang X, Mitchell C, Kliewer MA, Dempsey RJ. Methods for robust in vivo strain estimation in the carotid artery. Phys Med Biol. 2012; 57:7329–53. [PubMed: 23079725]
28. Shi H, Mitchell CC, McCormick M, Kliewer MA, Dempsey RJ, Varghese T. Preliminary in vivo atherosclerotic carotid plaque characterization using the accumulated axial strain and relative lateral shift strain indices. Phys Med Biol. 2008; 53:6377–94. [PubMed: 18941278]
29. Wang X, Jackson DC, Varghese T, Mitchell CC, Hermann BP, Kliewer MA, et al. Correlation of cognitive function with ultrasound strain indices in carotid plaque. Ultrasound Med Biol. 2014; 40:78–89. [PubMed: 24120415]
30. Rocque BG, Jackson D, Varghese T, Hermann B, McCormick M, Kliewer M, et al. Impaired cognitive function in patients with atherosclerotic carotid stenosis and correlation with ultrasound strain measurements. J Neurol Sci. 2012; 322:20–4. [PubMed: 22658531]
31. Falk E, Shah PK, Fuster V. Coronary plaque disruption. Circulation. 1995; 92:657–71. [PubMed: 7634481]
32. Gertz SD, Roberts WC. Hemodynamic shear force in rupture of coronary arterial atherosclerotic plaques. Am J Cardiol. 1990; 66:1368–72. [PubMed: 2244569]
33. Cinthio M, Ahlgren AR, Bergkvist J, Jansson T, Persson HW, Lindstrom K. Longitudinal movements and resulting shear strain of the arterial wall. Am J Physiol Heart Circ Physiol. 2006; 291:H394–402. [PubMed: 16473960]
34. McCormick M, Varghese T. An approach to unbiased subsample interpolation for motion tracking.
35. McCormick M, Rubert N, Varghese T. Bayesian regularization applied to ultrasound strain imaging. IEEE Trans Biomed Eng. 2011; 58:1612–20. [PubMed: 21245002]
36. Randolph C, Tierney MC, Mohr E, Chase TN. The Repeatable Battery for the Assessment of Neuropsychological Status (RBANS): preliminary clinical validity. J Clin Exp Neuropsychol. 1998; 20:310–9. [PubMed: 9845158]
37. Duff K, Patton D, Schoenberg MR, Mold J, Scott JG, Adams RL. Age- and education-corrected independent normative data for the RBANS in a community dwelling elderly sample. Clin Neuropsychol. 2003; 17:351–66. [PubMed: 14704885]
38. Ge W, Krueger CG, Weichmann A, Shanmuganayagam D, Varghese T. Displacement and strain esti- mation for evaluation of arterial wall stiffness using a familial hypercholesterolemia swine model of atherosclerosis. Med Phys. 2012; 39:4483–92. [PubMed: 22830780]
39. Hiyama T, Tanaka T, Endo S, Komine K, Kudo T, Kobayashi H, et al. Angiogenesis in atherosclerotic plaque obtained from carotid endarterectomy: association between symptomatology and plaque morphology. Neurol Med Chir (Tokyo). 2010; 50:1056–61. [PubMed: 21206178]
40. ten Kate GL, Sijbrands EJ, Valkema R, ten Cate FJ, Feinstein SB, van der Steen AF, et al. Molecular imaging of inflammation and intraplaque vasa vasorum: a step forward to identification of vulnerable plaques? J Nucl Cardiol. 2010; 17:897–912. [PubMed: 20552308]
41. Lawrence-Brown M, Stanley BM, Sun Z, Semmens JB, Liffman K. Stress and strain behaviour modelling of the carotid bifurcation. ANZ J Surg. 2011; 81:810–6. [PubMed: 22295401]
42. Idzenga T, Pasterkamp G, de Korte C. Shear strain in the adventitial layer of the arterial wall facilitates development of vulnerable plaques. Bioscience Hypotheses. 2009; 2:339–42.
43. Lusby RJ, Ferrell LD, Ehrenfeld WK, Stoney RJ, Wylie EJ. Carotid plaque hemorrhage. Its role in production of cerebral ischemia. Arch Surg. 1982; 117:1479–88. [PubMed: 6182861]
44. McCarthy MJ, Loftus IM, Thompson MM, Jones L, London NJ, Bell PR, et al. Angiogenesis and the atherosclerotic carotid plaque: an association between symptomatology and plaque morphology. J Vasc Surg. 1999; 30:261–8. [PubMed: 10436445]
45. Vicenzini E, Giannoni MF, Puccinelli F, et al. Detection of carotid adventitial vasa vasorum and plaque vascularization with ultrasound cadence contrast pulse sequencing technique and echo-contrast agent. Stroke. 2007; 38:2841–3. [PubMed: 17761913]

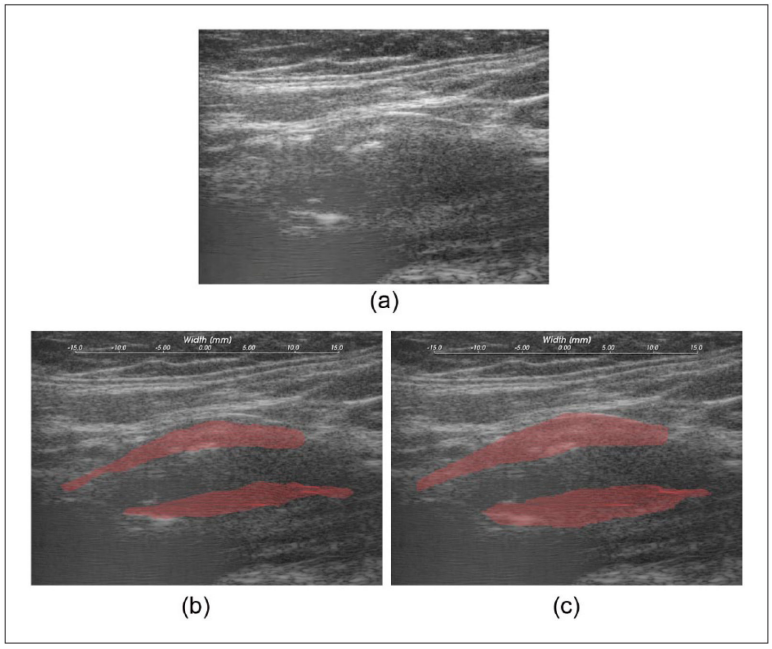

Figure 1.

B-mode image (a) and segmented plaque on B-mode image using the plaque-only segmentation (b) and the plaque-with-adventitia segmentation (c).

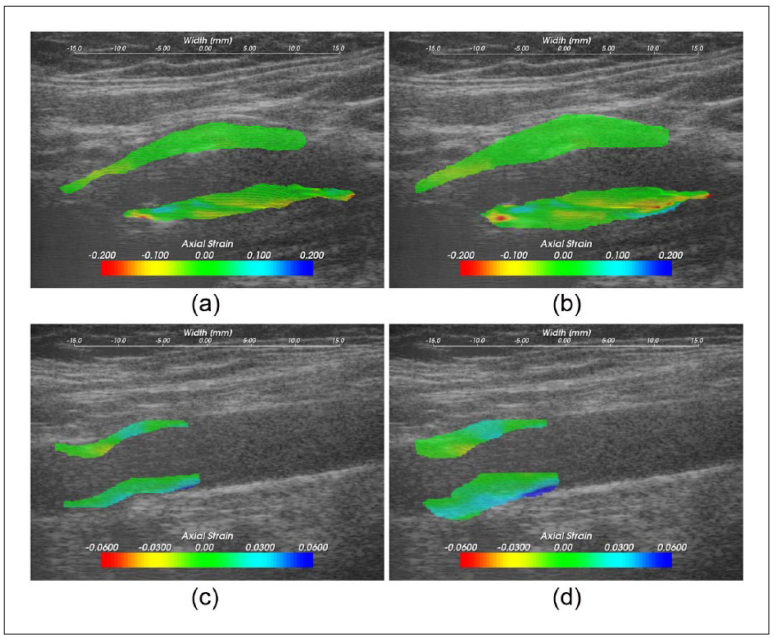

Figure 2.

Axial strain values overlaid on the B-mode image on a symptomatic plaque, (a) and (b), and an asymptomatic plaque, (c) and (d); (a) and (c) were using the plaque-only segmentation, and (b) and (d) the plaque-with-adventitia segmentation.

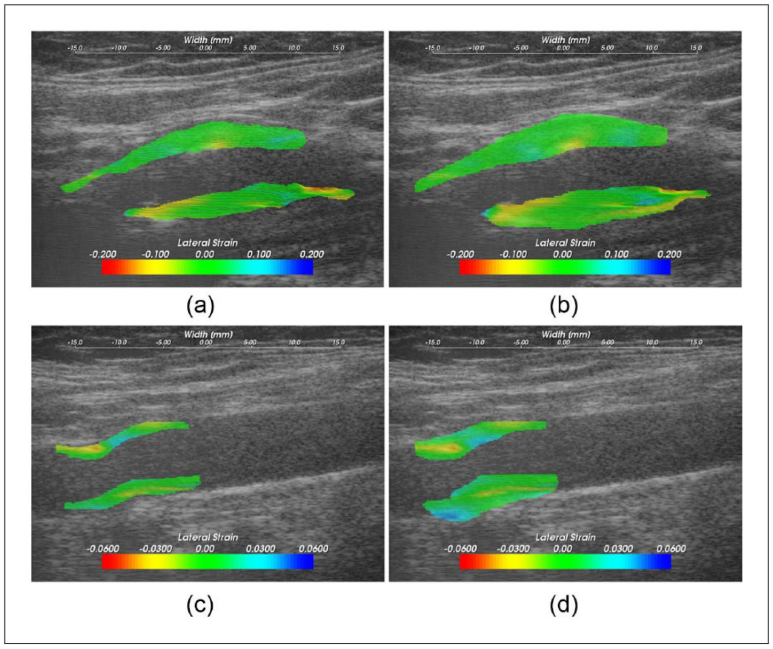

Figure 3.

Lateral strain values overlaid on the B-mode image on a symptomatic plaque, (a) and (b), and an asymptomatic plaque, (c) and (d); (a) and (c) were using the plaque-only segmentation, and (b) and (d) the plaque-with-adventitia segmentation.

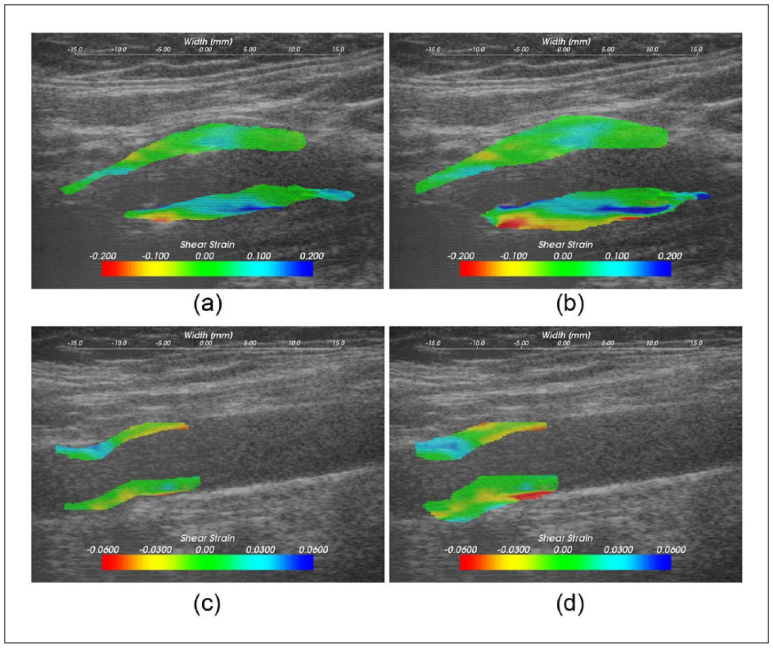

Figure 4.

Shear strain values overlaid on the B-mode image on a symptomatic plaque, (a) and (b), and an asymptomatic plaque, (c) and (d); (a) and (c) were using the plaque-only segmentation, and (b) and (d) the plaque-with-adventitia segmentation.

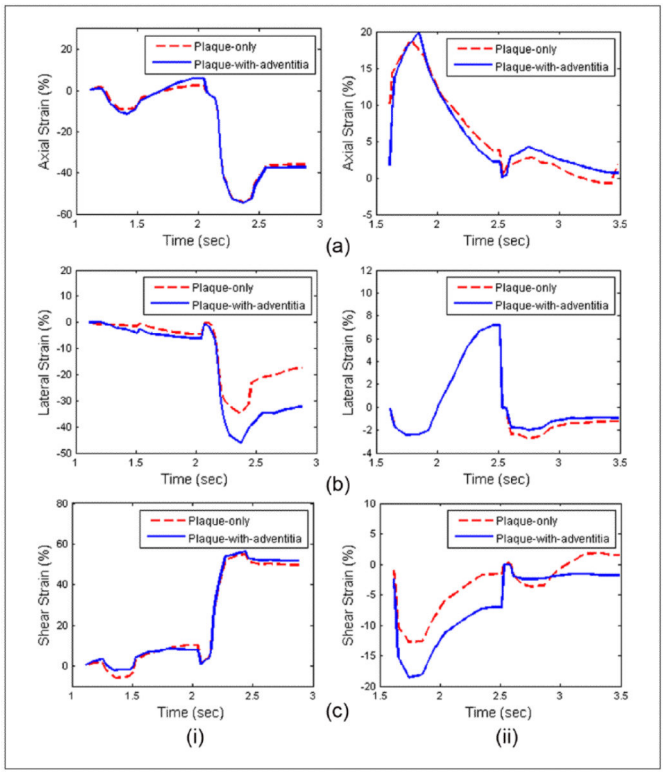

Figure 5.

Accumulated axial (a), lateral (b), and shear (c) strain over two cardiac cycles with plaque-only and plaque-with-wall segmentation on a symptomatic (i) and an asymptomatic (ii) patient.

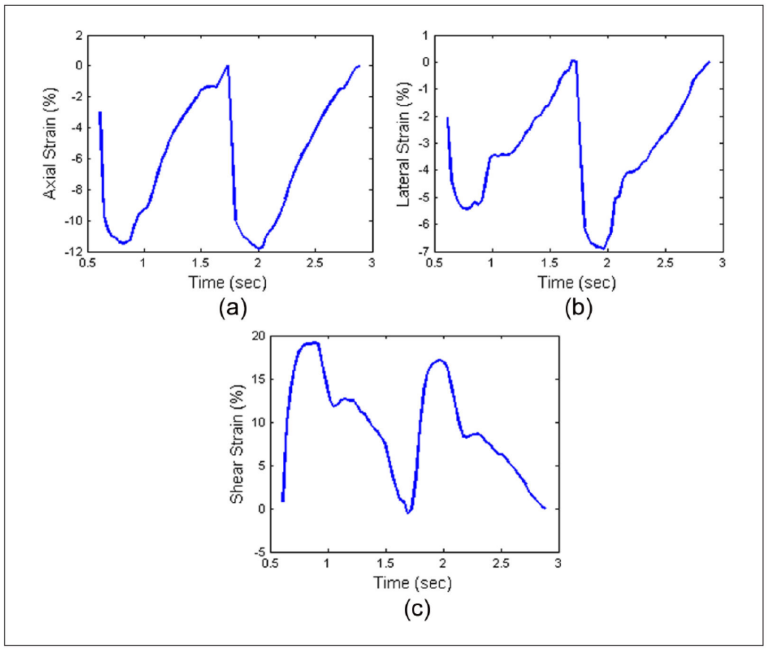

Figure 6.

Accumulated axial (a), lateral (b), and shear (c) strain over two cardiac cycles in carotid artery wall on a healthy human volunteer.

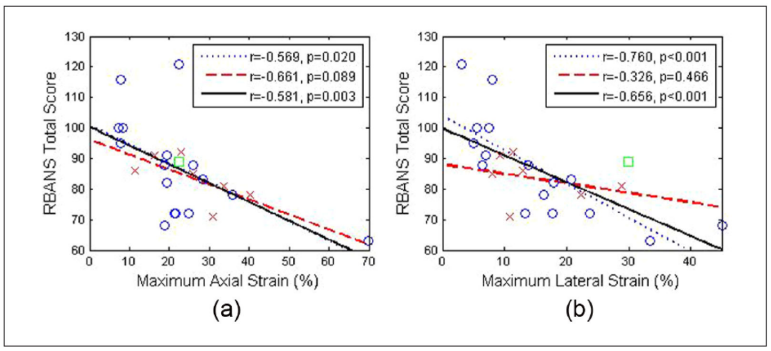

Figure 7.

Linear least-squares fits of RBANS Total score with maximum axial (a), and maximum lateral (b) strain averaged over the small region of interest. ○ = Symptomatic; x = asymptomatic; □ = uncertain; the dotted line represents the linear fit for symptomatic, the dashed line the linear fit for asymptomatic, and the solid line denotes the linear fit for all patients combined; RBANS = Repeatable Battery for the Assessment of Neuropsychological Status.

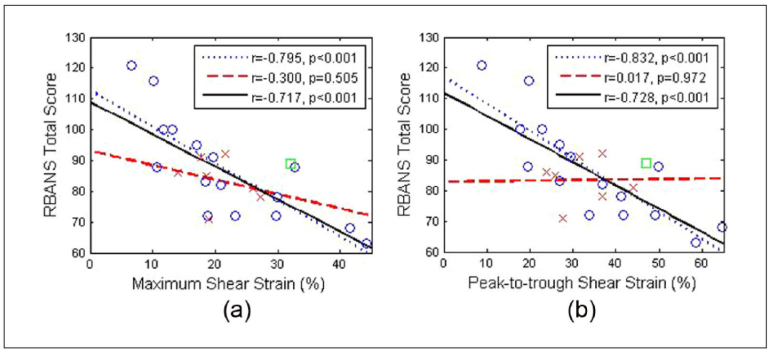

Figure 8.

Linear least-squares fits of RBANS Total score with maximum (a), and peak-to-trough (b) shear strain averaged over the small region of interest. ○ = Symptomatic; x = asymptomatic; □ = uncertain; the dotted line represents the linear fit for symptomatic, the dashed line the linear fit for asymptomatic, and the solid line denotes the linear fit for all patients combined; RBANS = Repeatable Battery for the Assessment of Neuropsychological Status.

Table 1

Correlations of RBANS Total Score for Plaque-Only and Plaque-with-Adventitia Segmentation.

	Maximum Axial Strain	Maximum Lateral Strain	Maximum Shear Strain
RBANS Total (Plaque-only)			
Symptomatic	**$r = -0.533$, $p = 0.032$**	**$r = -0.650$, $p = 0.006$**	$r = -0.432$, $p = 0.092$
Asymptomatic	$r = -0.530$, $p = 0.205$	$r = -0.115$, $p = 0.803$	$r = 0.037$, $p = 0.937$
All	**$r = -0.491$, $p = 0.014$**	**$r = -0.501$, $p = 0.012$**	$r = -0.345$, $p = 0.097$
RBANS Total (Plaque-with-adventitia)			
Symptomatic	**$r = -0.569$, $p = 0.020$**	**$r = -0.760$, $p < 0.001$**	**$r = -0.795$, $p < 0.001$**
Asymptomatic	$r = -0.661$, $p = 0.089$	$r = -0.326$, $p = 0.466$	$r = -0.300$, $p = 0.505$
All	**$r = -0.581$, $p = 0.003$**	**$r = -0.656$, $p < 0.001$**	**$r = -0.717$, $p < 0.001$**

Significant correlations are marked in bold. RBANS = Repeatable Battery for the Assessment of Neuropsychological Status.

Table 2

Correlations of the Specific Component Scores in RBANS Total with Maximum Strain Indices.

	Maximum Axial Strain	Maximum Lateral Strain	Maximum Shear Strain
Immediate memory			
Symptomatic	**$r = -0.592$, $p = 0.014$**	**$r = -0.740$, $p < 0.001$**	**$r = -0.752$, $p < 0.001$**
Asymptomatic	**$r = -0.852$, $p = 0.008$**	$r = -0.568$, $p = 0.167$	$r = -0.722$, $p = 0.052$
All	**$r = -0.620$, $p = 0.001$**	**$r = -0.566$, $p = 0.004$**	**$r = -0.602$, $p = 0.002$**
Visuospatial/constructional			
Symptomatic	$r = -0.191$, $p = 0.476$	**$r = -0.575$, $p = 0.018$**	**$r = -0.611$, $p = 0.011$**
Asymptomatic	$r = 0.195$, $p = 0.670$	$r = -0.047$, $p = 0.919$	$r = 0.266$, $p = 0.557$
All	$r = -0.162$, $p = 0.448$	**$r = -0.506$, $p = 0.011$**	**$r = -0.521$, $p = 0.009$**
Language			
Symptomatic	$r = -0.321$, $p = 0.222$	$r = -0.202$, $p = 0.452$	$r = -0.258$, $p = 0.332$
Asymptomatic	$r = -0.143$, $p = 0.756$	$r = -0.509$, $p = 0.227$	$r = -0.022$, $p = 0.962$
All	$r = -0.187$, $p = 0.381$	$r = -0.158$, $p = 0.459$	$r = -0.132$, $p = 0.539$
Attention			
Symptomatic	$r = -0.044$, $p = 0.870$	$r = -0.077$, $p = 0.776$	$r = -0.056$, $p = 0.837$
Asymptomatic	**$r = -0.838$, $p = 0.011$**	$r = -0.303$, $p = 0.499$	**$r = -0.758$, $p = 0.036$**
All	$r = -0.083$, $p = 0.699$	$r = -0.090$, $p = 0.674$	$r = -0.095$, $p = 0.657$
Delayed memory			
Symptomatic	**$r = -0.609$, $p = 0.011$**	**$r = -0.762$, $p < 0.001$**	**$r = -0.744$, $p < 0.001$**
Asymptomatic	$r = -0.345$, $p = 0.438$	$r = 0.119$, $p = 0.796$	$r = 0.079$, $p = 0.864$
All	**$r = -0.549$, $p = 0.005$**	**$r = -0.559$, $p = 0.004$**	**$r = -0.604$, $p = 0.002$**

Significant correlations are marked in bold. RBANS = Repeatable Battery for the Assessment of Neuropsychological Status.